

The G Protein-Coupled Receptor Latrophilin-2, A Marker for Heart Development, Induces Myocardial Repair After Infarction

Choon-Soo Lee^{1,2}, Hyun-Jai Cho^{3,*}, Jin-Woo Lee^{1,2}, Hyun Ju Son^{1,2}, Jaewon Lee¹, Minjun Kang^{1,2}, Hyo-Soo Kim^{1,2}

¹Strategic Center of Cell & Bio Therapy, Seoul National University Hospital, Seoul, South Korea

²Department of Molecular Medicine and Biopharmaceutical Sciences, Graduate School of Convergence Science and Technology, and College of Medicine or College of Pharmacy, Seoul National University, Seoul, South Korea

³Department of Internal Medicine, Seoul National University Hospital, Seoul, South Korea

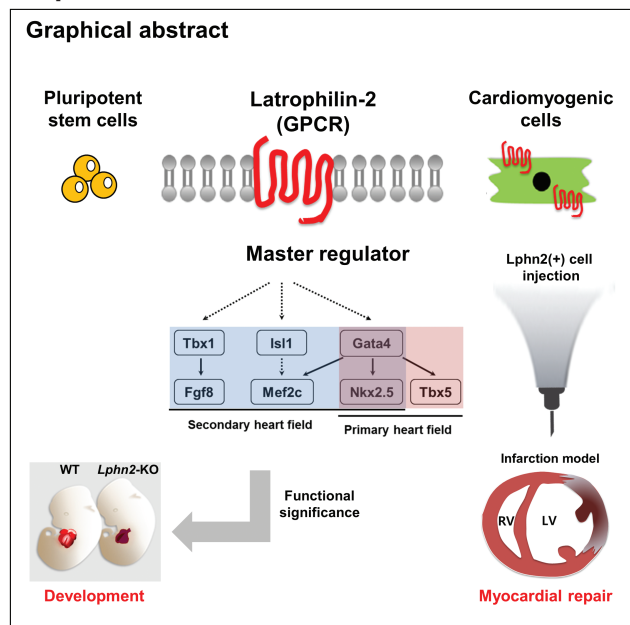
*Corresponding author: Hyun-Jai Cho, MD, Ph.D., Division of Cardiology, Department of Internal Medicine, Seoul National University Hospital, 101 Daehak-ro, Jongno-gu, Seoul 03080, South Korea. Tel: +82 2 2072 3931; Fax: +82 2 3675 0805. E-mail: hyunjaicho@snu.ac.kr; hyunjaicho@gmail.com

Abstract

Discovering cell–surface markers based on a comprehensive understanding of development is utilized to isolate a particular cell type with high purity for therapeutic purposes. Given that latrophilin-2 (Lphn2) substantially contributes to cardiac differentiation, we examined whether Lphn2 regulates functional significance in heart development and repair. We performed whole-mount immunostaining followed by clearing technique of embryo, RNA sequencing related to *Lphn2*-knockout (KO) embryo, and in vivo functional analyses of Lphn2+ cells using echocardiography. After immunostaining the cleared embryo sample, Lphn2 was exclusively observed in cardiac cells expressing α -sarcomeric actinin at embryonic days E9.5 and E10.5. Homozygous *Lphn2*-KO mice were embryonically lethal and showed underdevelopment of the ventricular myocardium. However, Lphn2 was not required to develop vessels, including endothelial cells and smooth muscle cells. For the purpose of cardiac regeneration, we transplanted pluripotent stem cell (PSC)-derived Lphn2+ cells into the infarcted heart. PSC-derived Lphn2+ cells differentiated into cardiomyocytes and regenerated the myocardium when transplanted into the infarcted heart, unlike Lphn2- cells. Transplanted Lphn2+ cells improved left-ventricle systolic function and reduced infarct size. We demonstrated that Lphn2 exhibits potential as a cardiomyogenic marker to facilitate targeted stem cell therapy for heart repair in clinical practice.

Key words: receptor; marker; heart development; embryo; infarction; regeneration.

Graphical Abstract



Abbreviations: PSC, pluripotent stem cell; CPC, cardiac progenitor cell; GPCR, G protein-coupled receptor; Lphn2, latrophilin-2; GFP, green fluorescent protein; KO, knockout

Received: 4 May 2021; Accepted: 13 October 2021.

© The Author(s) 2022. Published by Oxford University Press.

This is an Open Access article distributed under the terms of the Creative Commons Attribution-NonCommercial License (<https://creativecommons.org/licenses/by-nc/4.0/>), which permits non-commercial re-use, distribution, and reproduction in any medium, provided the original work is properly cited. For commercial re-use, please contact journals.permissions@oup.com.

Significance Statement

This study demonstrated that Lphn2 exhibits potential as a cardiomyogenic marker to facilitate targeted stem cell therapy for heart repair in clinical practice. The utilization of pluripotent stem cell-derived Lphn2+ cells could provide a targeted approach to regenerate myocardium after ischemic injury in clinical practice.

Introduction

Among cardiovascular diseases, ischemic heart failure, including myocardial infarction, is the most common, and its prevalence has been increasing.¹ Numerous studies have been conducted to overcome heart disease, but current medical treatment has a definite limitation to solve this global health issue.

In patients with myocardial infarction, the number of cardiomyocytes is significantly reduced due to cell death. Cardiomyocytes exist in a constant number over the life of a human being and have a slow dividing capacity of less than 1% per year and a limited ability to regenerate.² When the myocardium is damaged, there is no way to repair it other than externally supplying cardiomyocytes. It is challenging to deliver human pluripotent stem cell (PSC)-derived cardiomyocytes to the damaged heart, and the adult heart lacks endogenous cardiac stem and progenitor cells that can regenerate.^{3,4} Therefore, there has recently been an increasing demand for PSC-derived cardiomyocytes for cardiovascular disease and cell therapy studies.⁵

Recently, we identified cardiac-lineage markers, latrophilin-2 (Lphn2)^{6,7} and lysophosphatidic acid receptor 4 (LPA4)⁸ as G protein-coupled receptors (GPCRs). However, LPA4 expression was transient during cardiac differentiation from the undifferentiated state of PSCs. GPCRs are well-known to function in nervous system development and disease, metabolism, cancer.⁹⁻¹¹ GPCRs comprise the largest family of seven-transmembrane receptors, and there are more than 800 members of GPCRs discovered in humans.¹² In the case of adhesion GPCR, Lphn2 is separately classified as subfamily B2 due to its GPCR autoproteolysis-inducing domain that can self-cleavage.¹³

The influence of specific GPCRs on stem cell therapy for heart repair in clinical practice has not been reported, although GPCRs are well-known regulators of cardiac function.¹⁴ Latrophilins include three adhesion GPCRs (Lphn1–Lphn3) that contain large extracellular sequences, a seven-TMR-domain typical of GPCRs, and a relatively long intracellular tail.

In this study, we demonstrate that Lphn2 is a functional marker of cardiomyocytes and heart development. Furthermore, we show that PSC-derived Lphn2+ cells have therapeutic potential for damaged hearts.

Materials and Methods

The data that support the findings of this study are available from the corresponding author upon reasonable request.

Actin-GFP iPS Cell Generation

Skin fibroblasts from *Actin*-promoter driven GFP TG mice (C57BL/6-Tg(CAG-EGFP)10sb/J) were cultured in DMEM (Invitrogen) high glucose supplemented with 10% FBS (Invitrogen), 1% antibiotic-antimycotic (Invitrogen) on the plate (5% CO₂, 37°C). FUW-based lentiviral vectors (FUW-tetO-OSKM: Oct4/Sox2/Klf4/C-Myc and M2rtTA; Addgene)

were transfected into 293T cells using PEI (polyethylenimine; Sigma). The viral medium was harvested at 48 h following transfection and filtered through 0.45- μ m pore filters. For concentration, viral supernatant was ultracentrifuged at 107170 g for 1.5 h at 4°C, and the pellets were resuspended in an appropriate transduction medium. Virus soup was used to transduce skin fibroblasts (isolated from *Actin*-promoter driven GFP TG mice) with polybrene (10 μ g/mL). Twenty-four hours after transduction, the mESC medium was replaced. The mESC medium was composed of DMEM (Invitrogen) with 2 mM L-glutamine, 10% FBS (Invitrogen), 0.1 mM β -mercaptoethanol (Sigma–Aldrich), 1% non-essential amino acids (Invitrogen), 50 IU/mL penicillin, 50 mg/mL streptomycin (Invitrogen), and 2000 U/mL (20 ng/mL) recombinant LIF (Millipore, Cat. #: ESG1107). To initiate reprogramming, the medium was changed to mESC medium containing 2 μ g/mL doxycycline. Media was changed daily until ES-like colony was formed. *Actin*-GFP iPSCs were cultured on a mitomycin C (Sigma–Aldrich)-treated MEF (ATCC, Cat. #: SCRC-1040) feeder layer in gelatin (Sigma–Aldrich)-coated tissue culture dishes at 37°C and 5% CO₂ in an air atmosphere.¹⁵

Induction of Myocardial Infarction and Cell Transplantation

To generate myocardial infarction, 8 weeks old athymic nude mice were anesthetized with zoletil (91 mg/kg, Virbac Laboratories) and xylazine (11.65 mg/kg, Bayer), intubated, and artificially ventilated (Harvard apparatus).¹⁶ The chest was opened and the left anterior descending branch was ligated using 8-0 polypropylene. Immediately after LAD ligation, 1×10^5 cells from the respective groups were directly injected into the peri-infarct area.¹⁶⁻¹⁹ The same volume of PBS was injected in an identical fashion as a control. After 14 days the mouse heart was evaluated by echocardiographic examination and harvested.

Statistical Analysis

SPSS version 18.0 (SPSS Inc.) was used for all statistical analyses. All experiments were performed at least three times independently. In all cases, multiple experiments were performed independently to verify the reproducibility. The number of samples (*n*) used in each experiment is indicated in the legend or shown in the figures. The results are presented as the mean \pm standard error of the mean. Statistical analyses between two groups were conducted using the unpaired *t*-test or the Mann–Whitney *U* test, as appropriate. Comparison of more than two groups was performed using a one-way ANOVA. If the *F* test results were <0.05 , *post hoc* comparisons were performed with the Bonferroni test. Statistical significance was defined as $P < .05$ and indicated as * $P < .05$, ** $P < .01$. For animal studies, the sample size for experiments was determined empirically based on previous studies to ensure appropriate statistical power. Mice in the study were randomly chosen for myocardial infarction. No animals were excluded from statistical analysis, and the investigators were blinded in the studies.

Results

Expression of Lphn2 in the Embryonic Development and Adult Cells and Tissues

To verify whether Lphn2 is a cardiac-specific marker during development, we assessed its expression in mouse embryos using the clearing technique.²⁰ After immersion in a solution with a refractive index matching that of the clearing in the hybrid system, the mouse embryo became transparent

(Fig. 1A). After immunostaining the transparent embryo sample, Lphn2 was exclusively stained in cardiac cells expressing α -sarcomeric actinin (α -SA) at embryonic day (E) 9.5 (Fig. 1B; Supplemental online Video 1) and E10.5 (Fig. 1C; Supplemental online Video 2). Lphn2 was stained in the ventricle and atrium at E9.5, whereas Lphn2 was present in all heart chambers at E10.5. Next, we isolated single adult cardiomyocytes from the left ventricle of the heart of

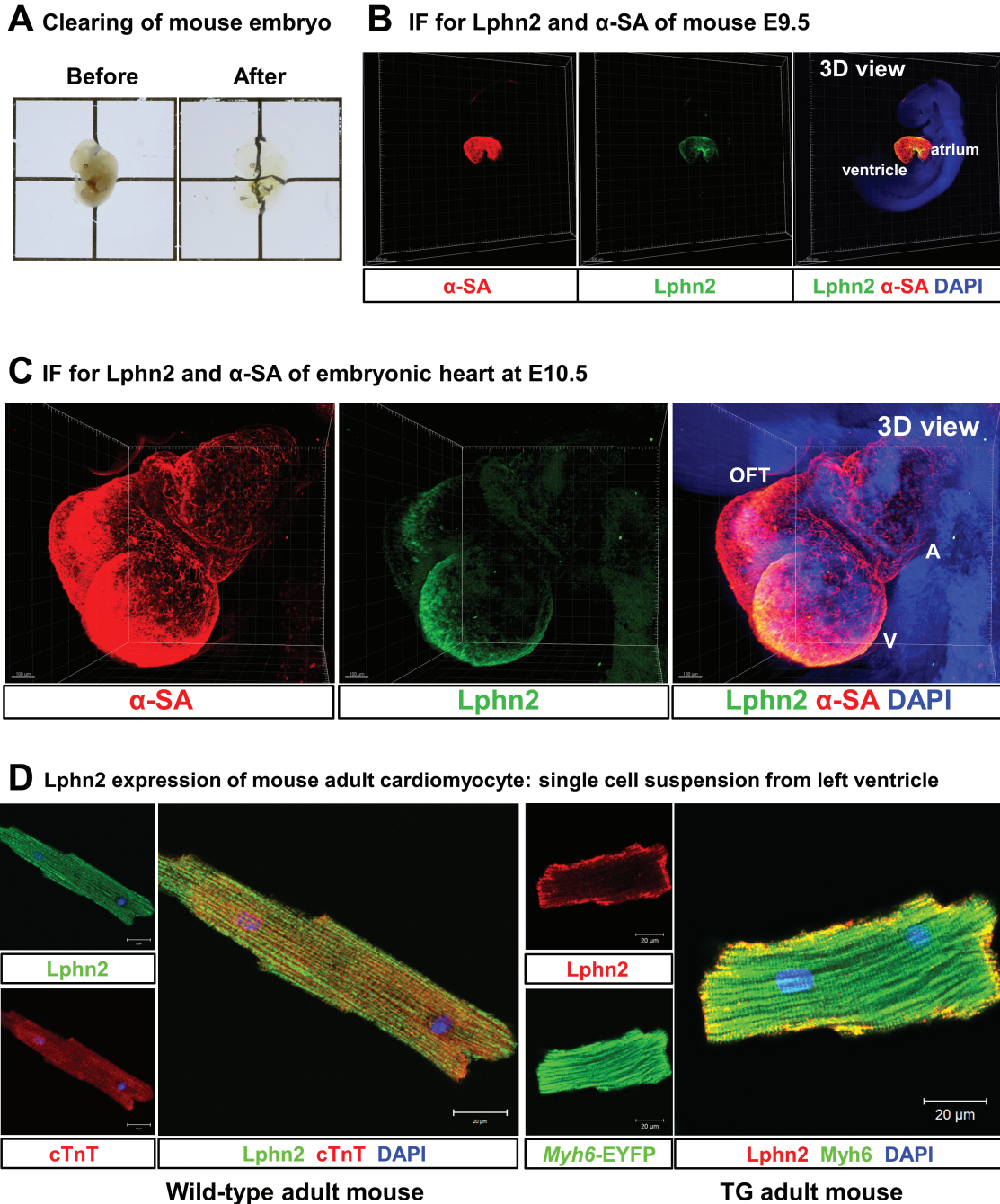


Figure 1. Lphn2 expression in mouse embryonic heart tissues, adult cardiomyocytes, and adult heart tissues. **(A):** Before and after images of a cleared mouse embryo (E10.5) prepared by fixing in paraformaldehyde, embedding in a hydrogel, electrophoretic tissue clearing, and refractive-index matching. **(B):** Three-dimensional rendering of a clearing-processed whole mouse embryo (E9.5), imaged by confocal microscopy for Lphn2 (green), α -SA (red), and merged expression. Blue, nuclear counterstain (DAPI). Scale bar, 500 μ m. **(C):** Immunostaining of a clearing-processed embryonic heart (E10.5) for Lphn2 (green) and α -SA (red). Blue, nuclear counterstain (DAPI). Scale bar, 200 μ m. OFT, outflow tract; V, ventricle; A, atrium. **(D)** Cytospin/immunostaining for Lphn2 in adult cardiomyocytes extracted by the Langendorff perfusion method from wild-type mice and *Myh6* promoter-driven EYFP mice. Blue, nuclear counterstain (DAPI).

wild-type C57BL/6 mice and transgenic mice expressing enhanced yellow fluorescence protein (EYFP) under the alpha myosin heavy chain (*Myh6*) promoter, using collagenase with the Langendorff perfusion system, and assessed *Lphn2* expression. Cardiomyocytes from the adult mouse heart expressed *Lphn2* on their surfaces (Fig. 1D).

We further analyzed the expression of *Lphn2* mRNA in various cell types. Of interest, the qPCR analysis revealed that *Lphn2* was highly expressed in mESC-derived cardiomyocytes as well as primary cultured neurons and neuronal stem cells (NSCs) (Supplementary Figure S1A). Consistent with our qPCR results, IF staining did not exhibit *Lphn2* expression in mouse Hepa1c1c7 or C2C12 cells; however, *Lphn2* was expressed only in the central nervous system (CNS)-related cells, including primary neurons and NSCs (Supplementary Figure S1B). Furthermore, since fibroblasts are converted to myofibroblasts in response to tissue injury or upon transforming growth factor (TGF)- β stimulation,²¹ we performed IF staining in primary-cultured cardiac fibroblasts to assess *Lphn2* expression. IF analysis revealed *Lphn2* expression neither in quiescent fibroblasts nor in myofibroblasts expressing smooth muscle actin (SMA) (Supplementary Figure S1C).

We also examined the heart after myocardial infarction and detected *Lphn2* expression on cardiomyocytes expressing α -SA in the peri-infarct area (Supplementary Figure S2A). Interestingly, *Lphn2*-positive cells did not express either SMA or isolectin B4 (ILB4), which are markers for vascular smooth muscle cells and endothelial cells, respectively (Supplementary Figure S2B). Previously, *Lphn2* was detected in multiple organ tissues of adult mice.²² We performed qPCR and western blotting analysis to confirm the gene and protein expression levels of *Lphn2*, respectively, in multiple adult organs. *Lphn2* was not detectable at the mRNA or protein level in most tissues but was enriched in the brain, heart, and lung (Supplementary Figure S3A, B). Also, we performed qPCR of embryonic and adult hearts to compare the expression patterns of *Lphn2*. Interestingly, a higher expression of *Lphn2* was found in the developing embryonic heart than in the adult heart, strongly suggesting a critical role of *Lphn2* in cardiogenesis (Supplementary Figure S4).

We then analyzed *LPHN2* expression in human heart tissues. IF staining demonstrated that *LPHN2* was present in cardiomyocytes (α -SA⁺), but not in smooth muscle cells (SMA⁺) or endothelial cells (UEA1-Lectin⁺) (Supplementary Figure S5). Taken together, these data indicate that *Lphn2* is highly expressed on cardiomyocytes and heart tissues in both mice and humans.

Lphn2 Shows Functional Significance as the Master Regulator of Heart-Development Genes

To examine the functional significance of *Lphn2* in development, we generated *Lphn2*-KO mice using *Lphn2*-KO ESCs. *Lphn2* heterozygous mice (*Lphn2*^{+/-}) were alive and fertile. When we tried to generate complete KO mice through the mating of *Lphn2*^{+/-} mice, the homozygous *Lphn2*-deficient fetus (*Lphn2*^{-/-}) was embryonically lethal after E15.5. We extracted total RNA from wild-type and *Lphn2* homo-KO (^{-/-}) embryos at E9.5 and performed RNA sequencing (RNA-Seq) analysis to explore gene expression differences associated with defects in heart development (Supplementary Figure S6). Intriguingly, most genes associated with heart development were downregulated in *Lphn2*^{-/-} embryos (Fig. 2A). The expression of genes responsible for atrioventricular valve

morphogenesis, embryonic heart tube development, outflow tract morphogenesis, and ventricular cardiac muscle tissue morphogenesis was lower in *Lphn2*^{-/-} embryos than in wild-type embryos (Fig. 2B).

To examine the use of *Lphn2* as a bona fide CPC marker during heart development, we assessed *Lphn2* expression during early embryonic development. The heart of *Lphn2*^{-/-} embryos at E11.5 exhibited underdevelopment of the ventricular myocardium and disrupted conotruncal development without any abnormality in the atrial chambers. Also, its *Gata4* expression was not as high as that in wild-type embryos (Fig. 3A). Furthermore, at E14.5, unlike the hearts of wild-type, those of *Lphn2*^{-/-} embryos revealed extensive underdevelopment of the myocardium, such that endocardial trabeculation was not visible (Fig. 3B). Conotruncal septation was also affected, and the endocardial cushion tissue at the aortic and pulmonary valves was not separated from the surrounding myocardium. Again, the right and left atrial myocardium and chambers were well developed, and the aorta and pulmonary trunks were also well-formed (Fig. 3B). After immunostaining of the cleared wild-type embryo, *Lphn2* was exclusively observed in the four cardiac chambers and outflow tract expressing α -SA at E14.5 (Fig. 3C; Supplemental online Video 3). However, *Lphn2*^{-/-} embryos exhibited abnormal heart development, with smaller ventricular mass at E14.5 (Fig. 3C; Supplemental online Video 4).

Next, we determined whether *Lphn2* is involved in the development of other tissues, including vessels, neurons, and the liver. No differences were observed in SMA expression in vascular smooth muscle cells or ILB4 in endothelial cells among wild-type, *Lphn2*^{+/-}, and *Lphn2*^{-/-} embryos (Fig. 4A, B). There were no differences in the ectoderm (neuron, β III-tubulin) and endoderm (liver, HepPar1) development among wild-type, *Lphn2*^{+/-}, and *Lphn2*^{-/-} embryos (Fig. 4C, D), demonstrating that *Lphn2* is not required for the development of other tissues, including vessels. We additionally performed immunofluorescent staining to validate the ectoderm expression during the embryonic development. As expected, there were no differences in Glial Fibrillary Acidic Protein (GFAP) expression of neuronal astrocytes in the brain among wild-type, *Lphn2*^{+/-}, and *Lphn2*^{-/-} embryos (Supplementary Figure S7A). There were also no differences in the endoderm (liver, albumin) development among wild-type, *Lphn2*^{+/-}, and *Lphn2*^{-/-} embryos (Supplementary Figure S7B). In addition, we performed the additional qPCR experiment to validate the reproducibility of the IF data for a subset of ectoderm-related genes (*NeuroD1*, *GFAP*, *Nestin*, and *Dab2*) or endoderm-related genes (*ALB*, *AFP*, *Foxa2*, and *Ihh*) in whole-body tissue at embryonic day 13.5. qPCR analysis showed that there was no significant difference between the 3 groups (WT embryo vs. *Lphn2*-hetero KO embryo vs. *Lphn2*-homo KO embryo) (Supplementary Figure S8).

Collectively, these data indicate that *Lphn2*-expressing CPCs play a significant role in generating the heart, acting as cardiac muscle progenitors that play roles different than those of previously described multipotent CPCs.²³⁻²⁶

Lphn2 has Therapeutic Potential to Induce Myocardial Repair after Infarction

We investigated the in vivo differentiation potential and therapeutic efficacy of iPSC-derived *Lphn2*⁺ CPCs. To evaluate how *Lphn2*⁺ cells can engraft and survive into infarct hearts, we generated green fluorescent protein (GFP)-expressing

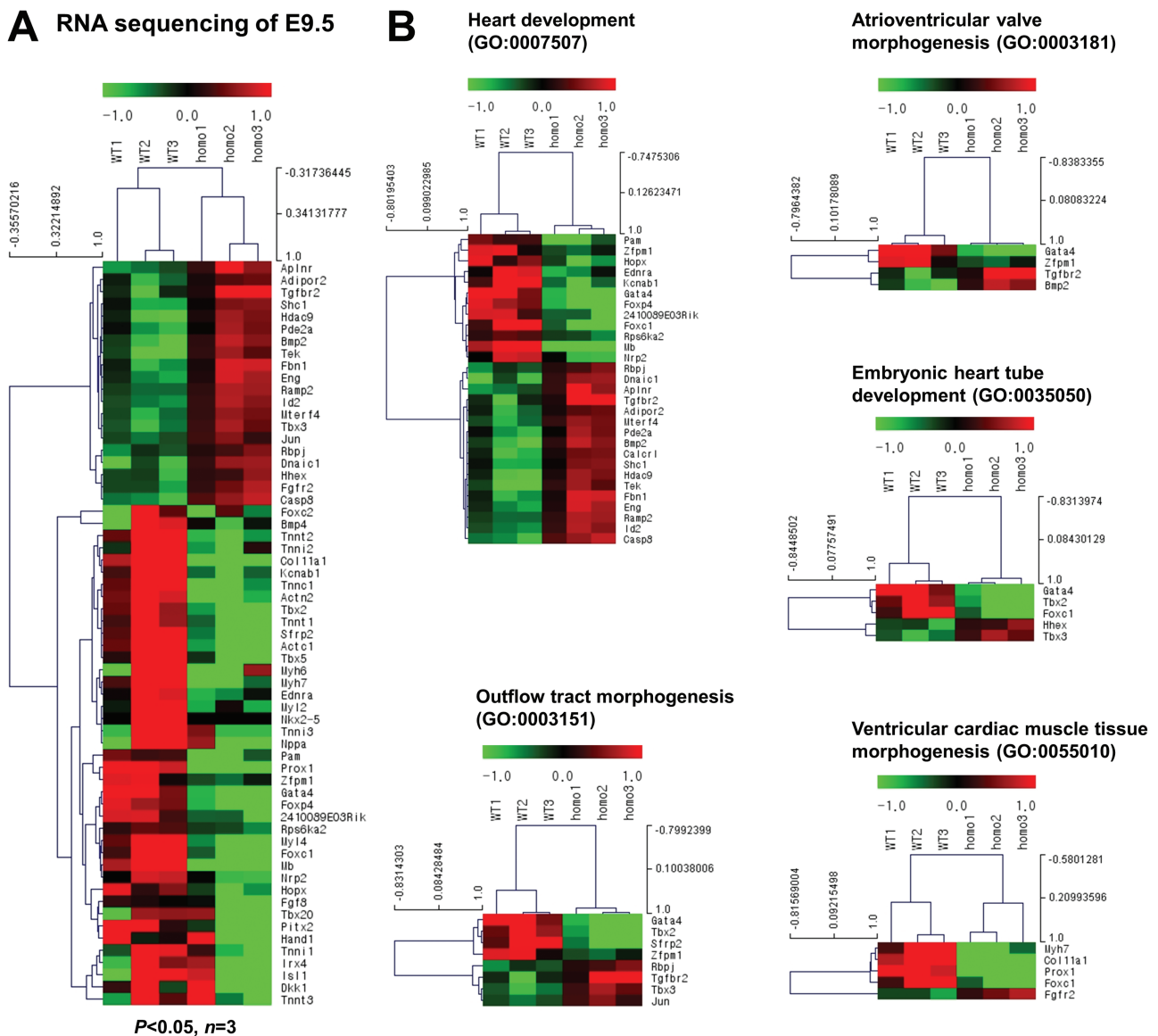


Figure 2. Expression of heart-specific genes by RNA sequencing method in *Lphn2* KO embryos. **(A):** RNA sequencing of whole embryonic tissues obtained from six samples of wild-type and *Lphn2*-homozygous ($-/-$) knockout embryos at E9.5 and gene clustering using MeV 4.9.0. Hierarchical cluster analyses were carried out with Euclidean distance correlation as the distance measurement with average linkage. Downregulated and upregulated genes in *Lphn2* $^{-/-}$ KO embryos are shown in green and red, respectively. Dysregulated genes with a >2-fold change in expression and with a *P*-value < .05 are shown (*n* = 3). **(B):** Heat map showing mRNA expression of gene ontology representing heart development, embryonic heart tube development, atrioventricular valve morphogenesis, outflow tract morphogenesis, and ventricular cardiac muscle tissue morphogenesis in six samples of wild-type and *Lphn2* $^{-/-}$ KO embryos at E9.5. To perform gene-annotation enrichment analysis, the genes were selected and input using the DAVID functional annotation tool.

iPSCs from the skin fibroblasts of *Actin* promoter-driven GFP transgenic mice (Fig. 5A). Upon sorting cells depending on the *Lphn2* and GFP expression after 7 days of differentiation of iPSCs toward CPCs, we could significantly attain enrichment of cardiac lineage cells in the *Lphn2* $^{+}$ population and exclusion of cardiac lineage cells from the *Lphn2* $^{-}$ cell population. *Lphn2* $^{+}$ cells at day 7 expressed cardiac lineage markers but did not contract spontaneously, indicating that the cells were in the CPC stage rather than being mature cardiomyocytes. Next, we induced myocardial infarction by ligating the left coronary artery, following which we injected 1×10^5 cells into the peri-infarct area.

Two weeks later, Masson's trichrome staining showed that the LV wall was replaced by a sizeable fibrotic scar and that

the LV dimension was markedly enlarged in the PBS-injected group (Fig. 5B). In contrast, the infarcted heart transplanted with *Lphn2* $^{+}$ cells showed several engrafted nodules that had replaced the LV wall and reduced the infarct size (Fig. 5B). Transplantation of *Lphn2* $^{+}$ cells significantly reduced the fibrosis area and length compared with those in the PBS-injected control group and *Lphn2* $^{-}$ cells (Supplementary Figure S9A). Echocardiography revealed significantly small LV dimensions at the systole and diastole, and the LV systolic function was higher in the *Lphn2* $^{+}$ cell group than in the PBS-injected control and *Lphn2* $^{-}$ cell groups (Fig. 5C).

Importantly, immunostaining analysis showed that transplanted GFP $^{+}$ /*Lphn2* $^{+}$ cells in the infarct zone were differentiated into α -SA $^{+}$ cardiomyocytes (Fig. 5D). Two weeks later,

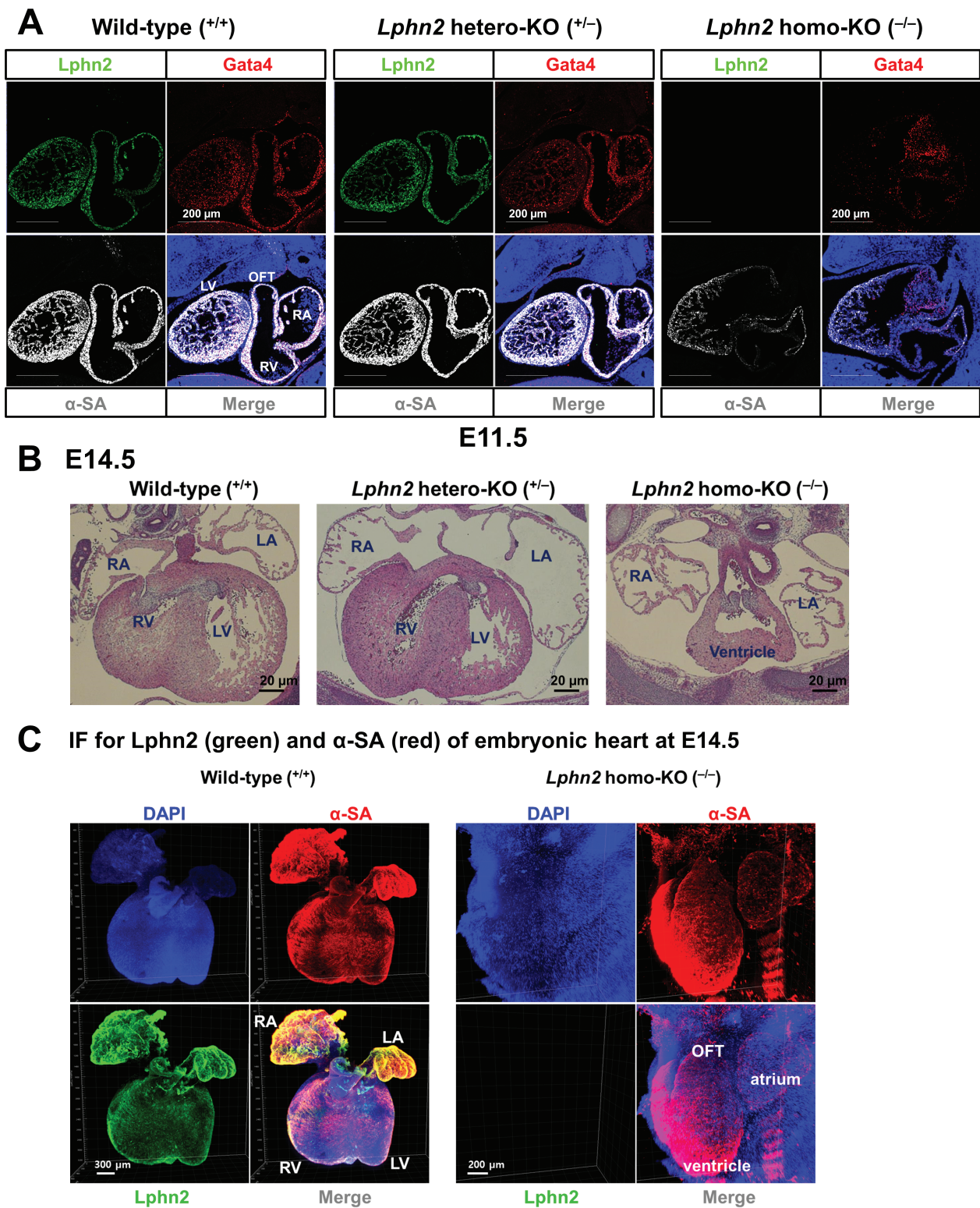


Figure 3. Functional significance of *Lphn2* in cardiac development. **(A):** Expression pattern of *Lphn2* overlap with early cardiac markers in heart development. Immunostaining of *Lphn2* (green), *Gata4* (red), and α-SA (white) in the heart of wild-type, *Lphn2*^{+/-}, and *Lphn2*^{-/-} embryos at E11.5. Blue, nuclear counterstain (DAPI). Scale bar, 200 μm. LV, left ventricle; OFT, outflow tract; RA, right atrium; RV, right ventricle. **(B):** Representative H&E-stained transverse sections revealed the disrupted conotruncal septation of ventricles in *Lphn2*^{-/-} KO embryos at E14.5. All embryos were from the same litter. Scale bars, 20 μm, LA, left atrium; LV, left ventricle; RA, right atrium; RV, right ventricle. **(C):** Immunostaining of a clearing-processed heart of wild-type and *Lphn2*^{-/-} KO embryos at E14.5 for *Lphn2* (green) and α-SA (red). Blue, nuclear counterstain (DAPI). LA, left atrium; RA, right atrium; LV, left ventricle; RV, right ventricle; OFT, outflow tract.

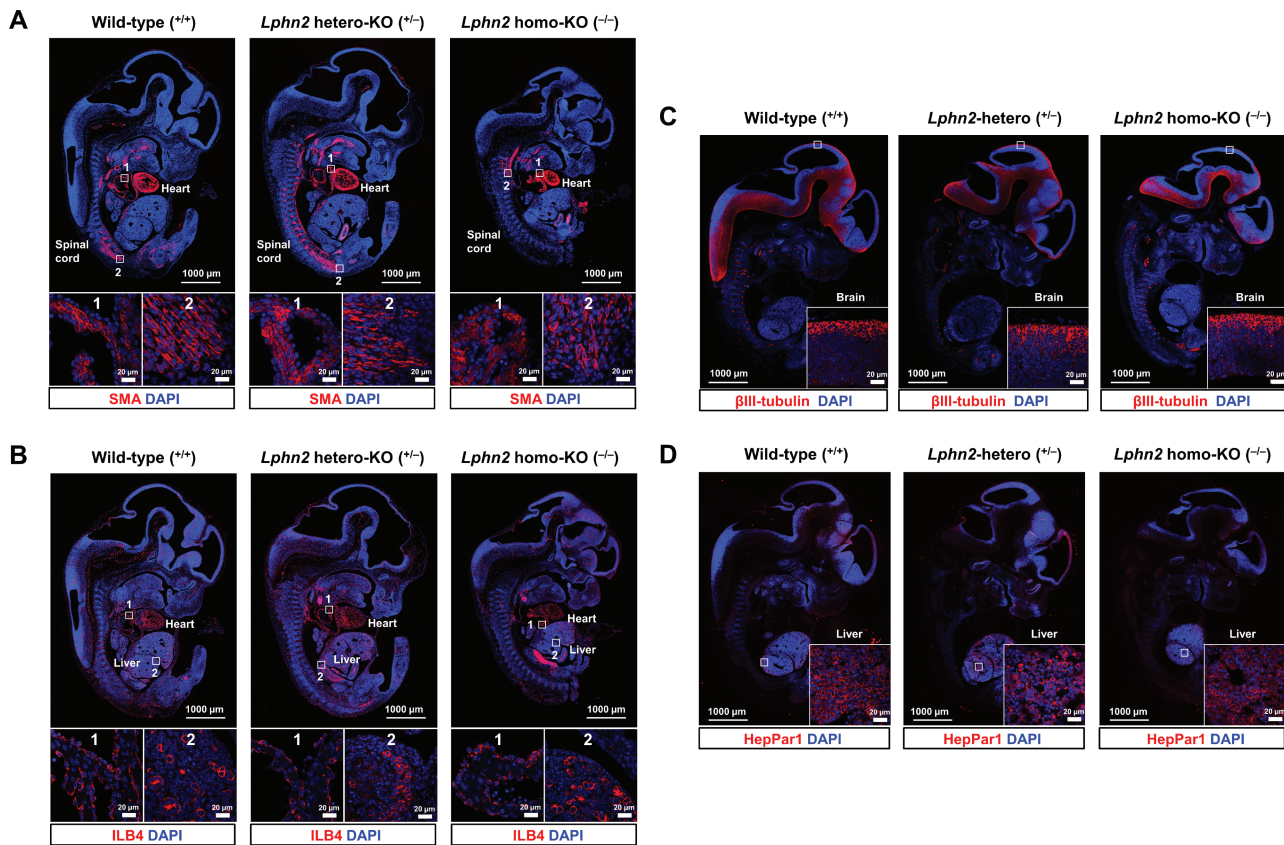


Figure 4. Role of *Lphn2* in mesodermal, ectodermal, and endodermal development of embryos. **(A, B):** Immunostaining of non-myogenic, vascular lineage markers SMA (A) and ILB4 (B) in wild-type and *Lphn2*-KO embryos at E11.5. Scale bars, 1000 μ m **(C):** Expression of β III-tubulin, an ectoderm lineage marker, in wild-type, *Lphn2*^{+/-} and *Lphn2*^{-/-} embryos at E11.5. **(D):** Expression of HepPar1, a hepatic endoderm marker, in wild-type, *Lphn2*^{+/-} and *Lphn2*^{-/-} embryos at E11.5. Scale bar, 20 μ m.

most GFP⁺/*Lphn2*⁺ cells expressed α -SA as a cardiac myocyte marker, but in unorganized patterns, implying that the engrafted cells were still CPCs or had differentiated into immature CMCs (Supplementary Figure S9B, C). Although GFP⁺/*Lphn2*⁻ cells successfully engrafted into the peri-infarct area, they did not differentiate into cardiomyocytes and did not improve the myocardial infarction (Fig. 5D; Supplementary Figure S9B, C). Immunostaining showed that grafted GFP⁺/*Lphn2*⁻ cells were primarily endoderm-lineage cells (Supplementary Figure S10A). Undifferentiated *Actin*-GFP-iPSCs formed large masses inside and outside the LV, reflecting the formation of a teratoma with the potential to differentiate into three germ layers (Supplementary Figures S10B, S11). In the PBS-injected control group, α -SA⁺ cardiomyocytes in the host myocardium of the peri-infarct zone expressed endogenous *Lphn2* at day 14 (Figure 5D; Supplementary Figure S9B, C).

Consequently, these findings suggest that PSC-derived *Lphn2*⁺ cells function as cardiomyogenic progenitor cells and may be viable candidates for the regeneration and repair of damaged hearts.

Discussion

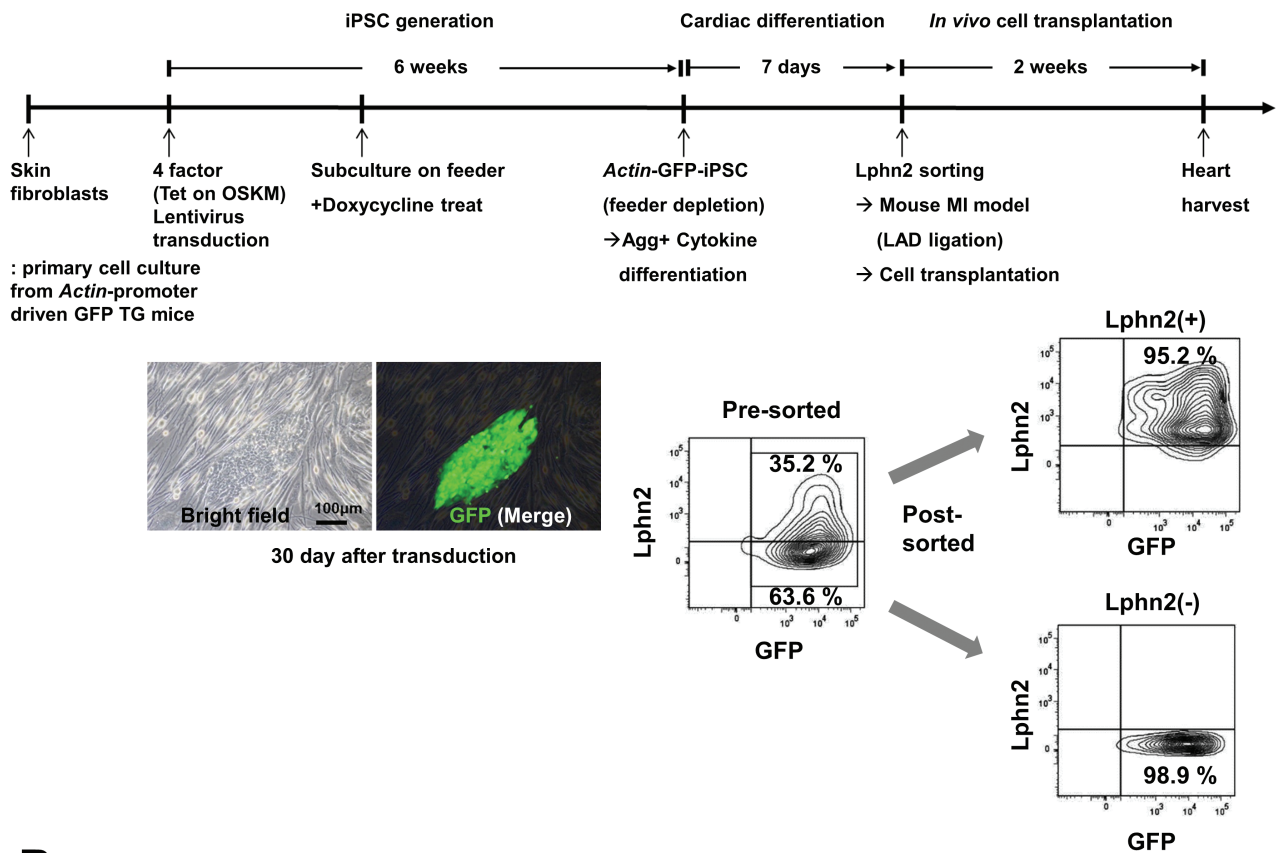
In this study, we confirmed that *Lphn2* is highly expressed in the mouse brain and heart. In our previous study, we found that *Lphn2* is a unique marker of cardiac progenitor cells and cardiomyocytes derived from PSCs.⁷ Although *Lphn2* has been implicated in the CNS, our study identified *Lphn2* as a

novel marker for cardiomyocytes in the embryonic and adult heart. Moreover, we demonstrated that *Lphn2* expression is more specific to the brain and heart, rather than ubiquitously expressed in adult tissues.

Unlike the previously reported ubiquitous expression throughout adult tissues,^{22,27} our qPCR analysis showed that *Lphn2* was highly expressed in both neuronal stem cells and primary cultured neurons. Also, IF staining of multiple cell types demonstrated that *Lphn2* expression did not appear in mouse Hepa1c1c7 and C2C12, but appeared only in primary neurons and neuronal stem cells. Of interest, *Lphn2* gene and protein were not detectable in most tissues but enriched in the brain, heart, and lung. In vivo, *Lphn2* was only expressed in the heart during the embryonic developmental stage, but in the adult, it was expressed in the brain as well. Thus, for the first time, we report the unverified functional role of *Lphn2* in heart development and adult damaged heart.

The clearing is a transparency technique of intact biological tissue using acrylamide-based hydrogels by removal of lipids.²⁰ Whole-mount embryo immunostaining with clearing showed that *Lphn2* is expressed in the heart with three-dimensional and topological morphologies during the developmental stage. Our clarified 3D images and movies show that four chambers expressed *Lphn2* of the heart are fully developed at E10.5 but not at E9.5. Since we established a powerful imaging analysis method with the clearing technique, it could be very informative to acquire 3D images of the heart in *Lphn2* homo-knockout embryos

A Schematic of GFP(+) iPSC derivation and *in vivo* cell transplantation after MI



B

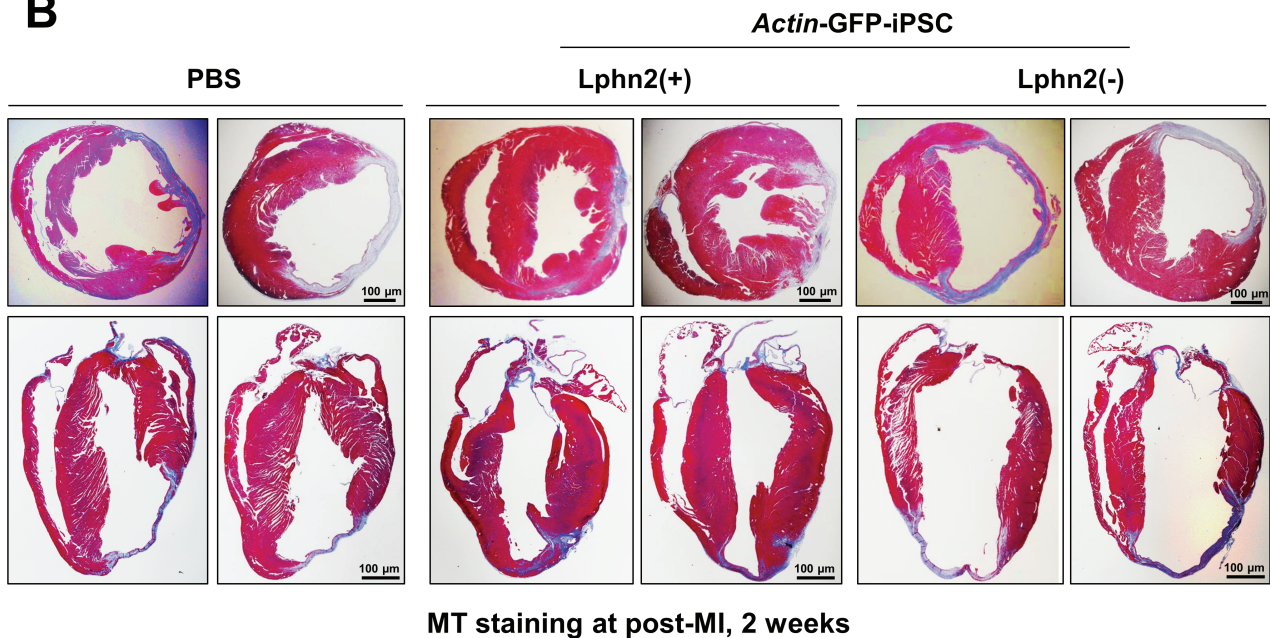
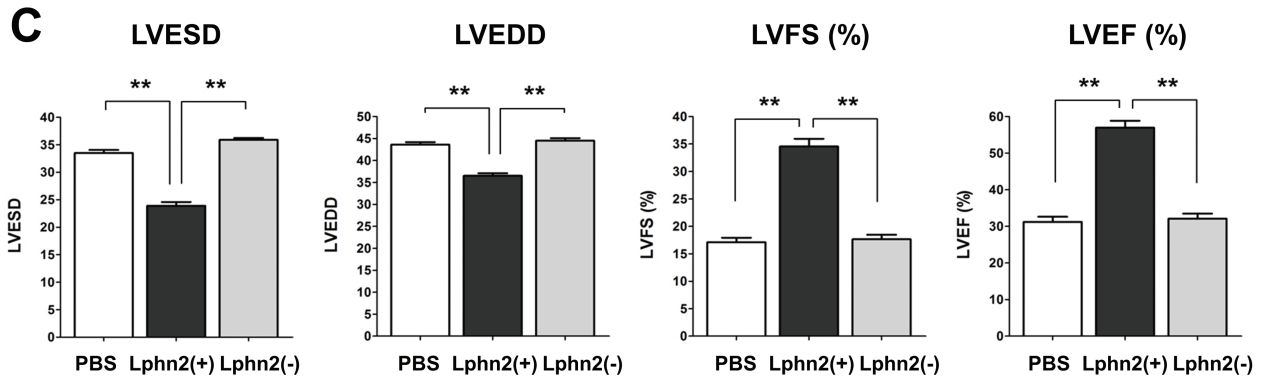


Figure 5. Therapeutic potential of Lphn2 to repair the heart after infarction. **(A):** Experimental scheme to assess the therapeutic efficacy of iPSC-derived Lphn2⁺ cells using a mouse myocardial infarction model. iPSCs were generated from primary skin fibroblasts isolated from *Actin*-GFP transgenic mice. iPSC-derived GFP⁺/Lphn2⁺ or GFP⁺/Lphn2⁻ cells were sorted at day 7 after cardiac differentiation and transplanted into the peri-infarct area. **(B):** Masson's trichrome staining was performed two weeks after the injection of PBS, iPSC-derived Lphn2⁺ cells, and Lphn2⁻ cells into the peri-infarct zone of the heart after ligation of the left coronary artery ($n = 15$ per group). **(C):** Echocardiographic parameters at 14 days after cell transplantation (** $P < .01$, ANOVA test and *post hoc* Bonferroni test, $n = 10$ per group). LVESD, LV end-systolic dimension; LVEDD, LV end-diastolic dimension; LVFS, LV fractional shortening; LVEF, LV ejection fraction. **(D):** Immunostaining of mouse myocardial infarction heart tissues injected with PBS, iPSC-derived Lphn2⁺ cells, and Lphn2⁻ cells. Injected GFP⁺ cells were traced and immunostained for GFP (green), Lphn2 (red), and α -SA (white). Blue, nuclear counterstain (DAPI). White rectangles in the upper images indicate regions shown at higher magnification from the lower image. Scale bars, 200 μ m (upper panels) or 50 μ m (lower panels).



D Tracing and differentiation of transplanted cells after myocardial infarction

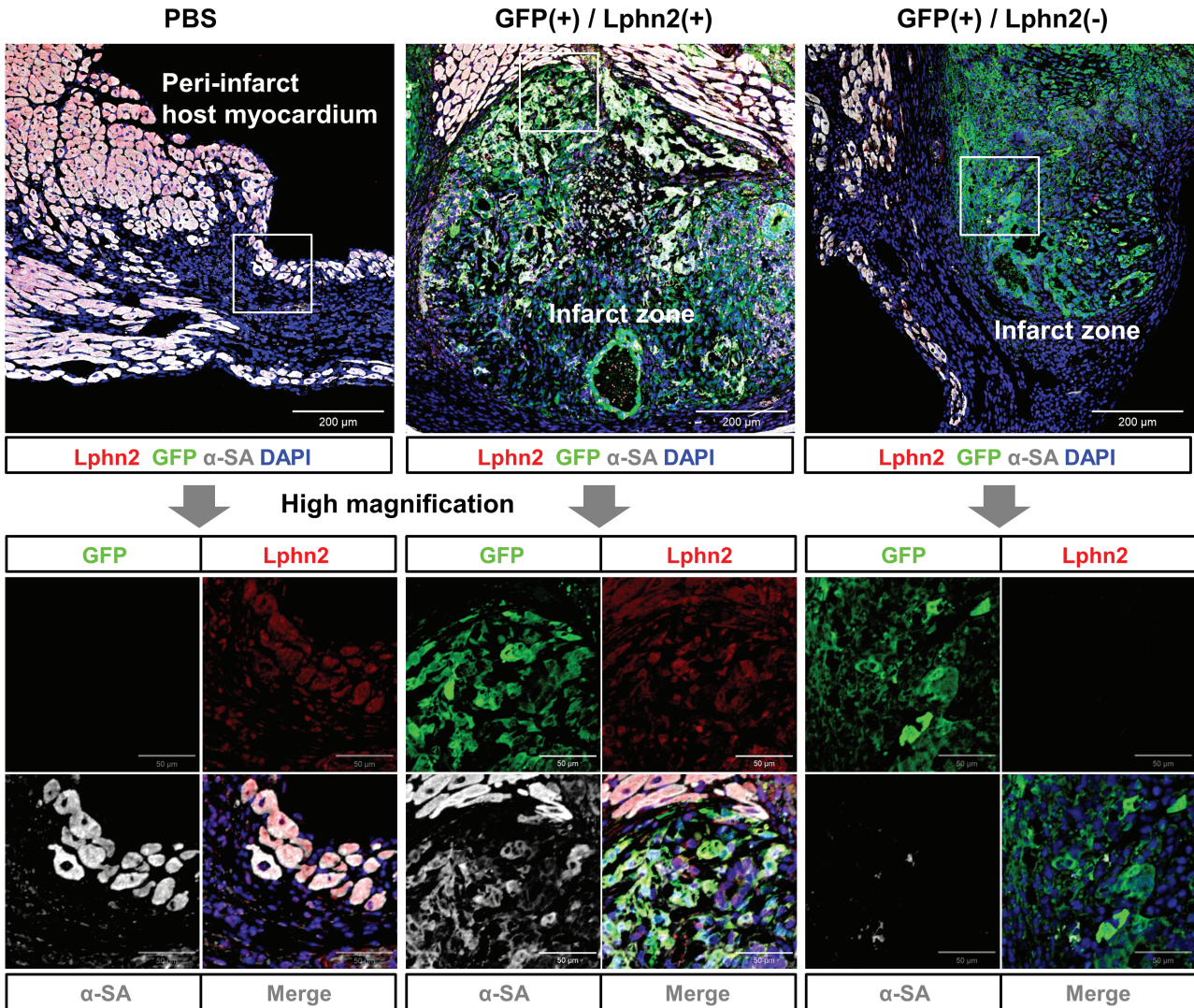


Figure 5. Continued

rather than 2D images of sections, which do not allow for accurate analysis of organ morphology. Therefore, we presume the spatial and temporal distributions of *Lphn2* follow a stepwise development of the heart. Furthermore, the gene expression patterns of RNA-Seq data for whole embryonic tissues from *Lphn2*^{-/-} mice support our findings of developmental defects, demonstrating that *Lphn2* is a

significant inducer of central transcription factors for heart development. These data indicate that *Lphn2* is a critical gene for cardiomyogenic progenitor cells and is essential for the successful development of embryos with fully mature cardiomyocytes.

Genetic mutations in *TBX5*, *NKX2-5*, and *GATA4* cause congenital heart diseases (CHDs) such as Holt-Oram

syndrome, atrial septal defects, and ventricular septal defects.²⁸⁻³⁰ Additionally, a recent study has shown that *TBX20*, which is known to interact with cardiac transcription factors such as *GATA4*, *NKX2-5*, and *TBX5*,³¹ is involved in the pathogenesis of left ventricular non-compaction cardiomyopathy.³² Our RNA-Seq analysis showed markedly reduced expression of *Gata4*, *Nkx2.5*, *Tbx5*, and *Tbx20* in *Lphn2*^{-/-} embryos, suggesting that there could be pathological implications in humans. Since mouse *Lphn2* is highly homologous to the human protein, our results have implications for congenital heart disease and regenerative cell therapy to restore lost cardiac muscles.

The present results suggesting that *Lphn2* is a therapeutic target in myocardial infarction are based on studies using *Lphn2*-KO mice. Therefore, the significance of *Lphn2* in the pathophysiology of heart disease should be further investigated in genetically modified models, such as in inducible cardiac-specific KO mice or heterozygous *Lphn2*-KO mice. These strategies will enable predicting which phenotype appears when *Lphn2* is knocked out at a particular developmental stage and how cardiac physiology changes when *Lphn2* is knocked out in the post-natal or adult stage. Further study is also needed to determine the phenotype under various physiological conditions, such as myocardial infarction in living and fertile heterozygous *Lphn2*-KO mice.

Conclusion

In summary, we have demonstrated that *Lphn2* exhibits potential as a cardiac-specific lineage marker to facilitate targeted stem cell therapy for heart repair. Furthermore, this study's results could be of potential use in regenerative medicine to restore cardiac muscle.

Acknowledgments

We thank Prof. Jeong-Wook Seo in the Department of Pathology at Seoul National University College of Medicine to evaluate and analyze mouse embryo samples. This research was supported by grants from the Korea Health Technology Research and Development Project "Strategic Center of Cell and Bio Therapy" (grant number: HI17C2085) and "Korea Research-Driven Hospital" (HI14C1277) through the Korea Health Industry Development Institute, funded by the Ministry of Health and Welfare, Korea.

Conflict of Interest

The authors declared no potential conflicts of interest.

Author Contributions

C.-S.L.: conception and design, collection and assembly of data, data analysis and interpretation, manuscript writing; H.-J.C.: conception and design, data analysis and interpretation, manuscript writing, financial support; J.-W.L.: collection and assembly of data, data analysis and interpretation; H.J.S.: data analysis and interpretation, manuscript writing; J.L.: collection and assembly of data; M.K.: collection and assembly of data; H-S.K.: conception and design, data analysis and interpretation, financial support.

Data Availability

The data that support the findings of this study are available from the corresponding author upon reasonable request.

References

- Braunwald E. The war against heart failure: the Lancet lecture. *Lancet*. 2015;385(9970):812-824.
- Galdos FX, Guo Y, Paige SL, et al. Cardiac regeneration: lessons from development. *Circ Res*. 2017;120(6):941-959.
- Blau HM, Daley GQ. Stem cells in the treatment of disease. *New Engl J Med*. 2019;380(18):1748-1760.
- Maliken BD, Molkentin JD. Undeniable evidence that the adult mammalian heart lacks an endogenous regenerative stem cell. *Circulation*. 2018;138(8):806-808.
- Matsa E, Burrige PW, Wu JC. Human stem cells for modeling heart disease and for drug discovery. *Sci Transl Med*. 2014;6(239):239ps-239p6.
- Lee CS, Cho HJ, Lee JW, et al. Identification of latrophilin-2 as a novel cell-surface marker for the cardiomyogenic lineage and its functional significance in heart development. *Circulation*. 2019;139(25):2910-2912.
- Lee CS, Cho HJ, Lee JW, et al. Adhesion GPCR latrophilin-2 specifies cardiac lineage commitment through CDK5, Src, and P38MAPK. *Stem Cell Rep*. 2021;16(4):868-882.
- Lee JW, Lee CS, Ryu YR, et al. Lysophosphatidic acid receptor 4 is transiently expressed during cardiac differentiation and critical for repair of the damaged heart. *Mol Ther*. 2021;29(3):1151-1163.
- Langenhan T, Piao X, Monk KR. Adhesion G protein-coupled receptors in nervous system development and disease. *Nat Rev Neurosci*. 2016;17(9):550-561.
- Olaniru OE, Persaud SJ. Adhesion G-protein coupled receptors: implications for metabolic function. *Pharmacol Ther*. 2019;198:123-134.
- Lappano R, Maggiolini M. G protein-coupled receptors: novel targets for drug discovery in cancer. *Nat Rev Drug Discov*. 2011;10(1):47-60.
- Fredriksson R, Lagerstrom MC, Lundin LG, et al. The G-protein-coupled receptors in the human genome form five main families. Phylogenetic analysis, paralogon groups, and fingerprints. *Mol Pharmacol*. 2003;63(6):1256-1272.
- Vizurraga A, Adhikari R, Yeung J, et al. Mechanisms of adhesion G protein-coupled receptor activation. *J Biol Chem*. 2020;295(41):14065-14083.
- Tilley DG. G Protein-dependent and G protein-independent signaling pathways and their impact on cardiac function. *Circ Res*. 2011;109(2):217-230.
- Cho HJ, Lee CS, Kwon YW, et al. Induction of pluripotent stem cells from adult somatic cells by protein-based reprogramming without genetic manipulation. *Blood*. 2010;116(3):386-395.
- Cho HJ, Lee HJ, Youn SW, et al. Secondary sphere formation enhances the functionality of cardiac progenitor cells. *Mol Ther*. 2012;20(9):1750-1766.
- Lee HJ, Cho HJ, Kwon YW, et al. Phenotypic modulation of human cardiospheres between stemness and paracrine activity, and implications for combined transplantation in cardiovascular regeneration. *Biomaterials*. 2013;34(38):9819-9829.
- Hodgson DM, Behfar A, Zingman LV, et al. Stable benefit of embryonic stem cell therapy in myocardial infarction. *Am J Physiol Heart Circ Physiol*. 2004;287(2):H471-H479.
- Li G, Chen J, Zhang X, et al. Cardiac repair in a mouse model of acute myocardial infarction with trophoblast stem cells. *Sci Rep*. 2017;7:44376.
- Chung K, Wallace J, Kim SY, et al. Structural and molecular interrogation of intact biological systems. *Nature*. 2013;497(7449):332-337.
- Leask A. Potential therapeutic targets for cardiac fibrosis: TGFbeta, angiotensin, endothelin, CCN2, and PDGF, partners in fibroblast activation. *Circ Res*. 2010;106(11):1675-1680.

22. Boucard AA, Maxeiner S, Sudhof TC. Latrophilins function as heterophilic cell-adhesion molecules by binding to teneurins: regulation by alternative splicing. *J Biol Chem*. 2014;289(1):387-402.
23. Kattman SJ, Huber TL, Keller GM. Multipotent flk-1+ cardiovascular progenitor cells give rise to the cardiomyocyte, endothelial, and vascular smooth muscle lineages. *Dev Cell*. 2006;11(5):723-732.
24. Moretti A, Caron L, Nakano A, et al. Multipotent embryonic isl1+ progenitor cells lead to cardiac, smooth muscle, and endothelial cell diversification. *Cell*. 2006;127(6):1151-1165.
25. Wu SM, Fujiwara Y, Cibulsky SM, et al. Developmental origin of a bipotential myocardial and smooth muscle cell precursor in the mammalian heart. *Cell*. 2006;127(6):1137-1150.
26. Sturzu AC, Wu SM. Developmental and regenerative biology of multipotent cardiovascular progenitor cells. *Circ Res*. 2011;108(3):353-364.
27. Anderson GR, Maxeiner S, Sando R, et al. Postsynaptic adhesion GPCR latrophilin-2 mediates target recognition in entorhinal-hippocampal synapse assembly. *J Cell Biol*. 2017;216(11):3831-3846.
28. Basson CT, Bachinsky DR, Lin RC, et al. Mutations in human TBX5 [corrected] cause limb and cardiac malformation in Holt-Oram syndrome. *Nat Genet*. 1997;15(1):30-35.
29. Schott JJ, Benson DW, Basson CT, et al. Congenital heart disease caused by mutations in the transcription factor NKX2-5. *Science*. 1998;281(5373):108-111.
30. Garg V, Kathiriyai IS, Barnes R, et al. GATA4 mutations cause human congenital heart defects and reveal an interaction with TBX5. *Nature*. 2003;424(6947):443-447.
31. Boogerd CJ, Zhu X, Aneas I, et al. Tbx20 is required in mid-gestation cardiomyocytes and plays a central role in atrial development. *Circ Res*. 2018;123(4):428-442.
32. Kodo K, Ong SG, Jahanbani F, et al. iPSC-derived cardiomyocytes reveal abnormal TGF-beta signalling in left ventricular non-compaction cardiomyopathy. *Nat Cell Biol*. 2016;18(10):1031-1042.